



## Shock Wave Propagation with Shear-layer and Surface Interaction during Transonic Deceleration

Irshaad Mahomed<sup>1,\*</sup>, Hamed Roohani<sup>1</sup>, Irvy M.A. Gledhill<sup>1</sup>, and Beric W. Skews<sup>1</sup>

1: School of Mechanical, Industrial, and Aeronautical Engineering, Faculty of Engineering, University of Witwatersrand, South Africa

\* Corresponding author: Irshaad.mahomed@wits.ac.za

**Keywords:** Shock shear layer Interaction, Shock boundary layer interaction, Numerical modelling, Unsteady flow, Accelerating flow

**ABSTRACT** Rapid deceleration through transonic Mach numbers in the order of 100g (where g is the acceleration due to gravity = 9.81 m.s<sup>-2</sup>) for two-dimensional aerofoil shapes RAE2022 and NACA0012 at zero incidence, demonstrated upstream bow shock motion which does not occur for the constant velocity case performed at the same instantaneous transonic flight Mach numbers (Roohani & Skews, 2009) and this was explained by the flow history effect. This was similarly observed for the wake shock from the transonic deceleration of a cone-cylinder at zero incidence (Mahomed, Roohani, Skews, & Gledhill, 2011).

The wake shock's foot, initially, is located upon the wake shear layer, and during transonic deceleration, this shock will propagate upstream on the wake shear layer towards the base and thereafter on the cylinder surface. The upstream motion of the wake shock on the shear layer and boundary layer will induce secondary waves that trail behind the wake shock. The wake shock strength determines the strength of the induced waves. Development of induced waves was not observed for the upstream propagation of the bow shock. The shock wave dynamics during deceleration have been extended to three-dimensional flow with selected results reported here about the secondary waves from upstream propagation of the wake shock, for a cone-cylinder at  $\alpha = 5^\circ$ .

Cone-cylinder deceleration was modelled numerically in ANSYS Fluent V.19 series using the Moving Reference Frame (MRF) acceleration technique. The cone-cylinder was decelerated from steady flight Mach number 1.10 until approximately 0.80 at 400g deceleration magnitude. The MRF acceleration technique solves the Navier-stokes equations in an absolute reference frame with results transformed to the relative, non-inertial reference frame. The Navier-stokes equations written in the absolute reference frame for an accelerating projectile is given in (Mahomed, Roohani, Skews, & Gledhill, 2011) and for general projectile motion in (Forsberg, Gledhill, Eliasson, & Nordström, 2003) and (Gledhill, et al., 2016), including a description of the transform between absolute and relative, non-inertial reference frames.

The solver is a finite volume URANS (Unsteady Reynolds Averaged Navier Stokes) implicit, density based, and second-order accurate, with Roe-Flux Difference Splitting scheme for spatial discretization and dual-time stepping for transient. The three-dimensional flow domain has a single symmetry plane and a pressure far field boundary condition located 20 body lengths away. The body length for the cone-cylinder is 270.6 mm, diameter 25 mm, and cone-half angle 10°.

Steady solver validation compared MRF with zero acceleration to wind tunnel experiments at flight Mach number 0.95 (Hsieh, 1975) and 1.5 (Hsieh, 1977). Unsteady solver validation compared MRF with velocity dependent drag to a ballistic range experiment. Additional detail of the validation and verification results for the steady and unsteady solvers are shown in (Mahomed, Roohani, Skews, & Gledhill, 2023) and (Mahomed, Roohani, Skews, & Gledhill, 2011), including the solver, turbulence model, and solution-based grid adaption.

During deceleration at 400g, from steady flight Mach number 1.10, the asymmetric bow shock propagates upstream when the flight Mach number has approached ~1.0, and this wave is followed by the wake shock. The wake shock is identified in Figs. 1 and 2 at  $M(t) = 0.95$  and 0.90 respectively, at two different locations with respect to the cylinder base. The wake shock propagates upstream from the shear layer towards the shoulder and thereafter, continues upstream away from the cone-cylinder.

The wake shock's foot locally modifies the curvature of the shear layer. This creates a trailing expansion wave. This is shown in Figs. 1 and 2. A trailing terminal shock develops if the trailing expansion is sufficiently strong. This creates an expansion-compression pair.

The wake shock's foot at the cylinder base creates a local surface compression which thickens the boundary layer. The thickened boundary layer develops a concave profile with an expansion region sufficiently strong to produce a trailing terminal

shock. The wake shock's strength reduces during upstream propagation. This will reduce the capability of the wake shock's foot to distort the boundary layer curvature. The flow history effect means that the trailing expansion and compression waves will not vanish once they have developed and instead will convect by propagating upstream and expanding radially outward.

Concluding aspects from this initial analysis are secondary waves does develop behind the wake shock during upstream propagation. The secondary waves are the trailing expansion and compression waves which, too, propagate upstream. There exists a possibility where these secondary waves may disrupt fin performance during deceleration. Further analysis considers  $\alpha$  up to  $15^\circ$ .

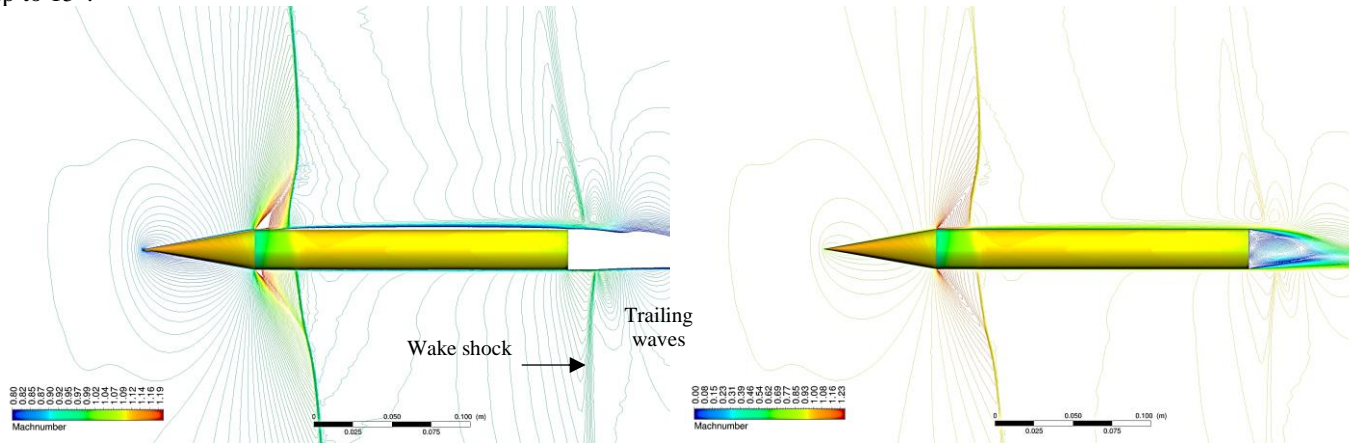


Figure 1. Symmetry plane contours at  $M(t) = 0.95$ , contour range reduced to show wake shock and secondary waves (left) and full range to show wake region (right). Deceleration 400g. Flow direction is left to right and wave propagation is right to left.

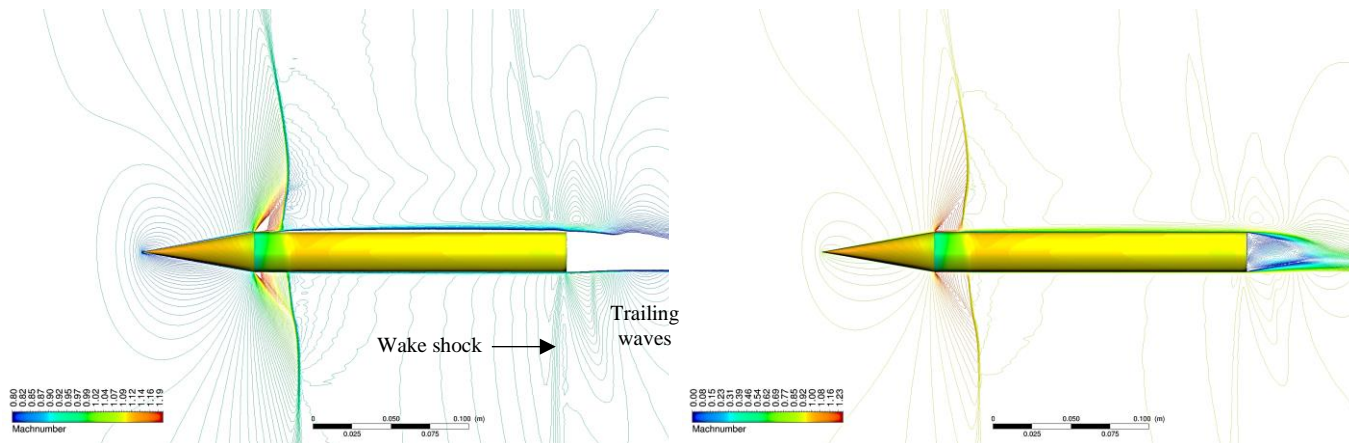


Figure 2. Symmetry plane contours at  $M(t) = 0.90$ , contour range reduced to show wake shock and secondary waves (left) and full range to show wake region (right). Deceleration 400g. Flow direction is left to right and wave propagation is right to left.

## 1 REFERENCES

- Forsberg, K., Gledhill, I.M.A., Eliasson, P., & Nordström, J. (2003). Investigations of acceleration effects on missile aerodynamics using CFD. *21st Applied Aerodynamics Conference*. Orlando, Florida: AIAA 2003-4084.
- Gledhill, I.M.A., Roohani, H., Forsberg, K., Eliasson, P., Skews, B.W., & Nordstrom, J. (2016). Theoretical treatment of fluid flow for accelerating bodies. *Theoretical and Computational Fluid Dynamics*, 30, 449-467.
- Hsieh, T. (1975). Flow-field about a hemisphere cylinder in the transonic and low supersonic Mach number range. *Arnold Engineering Development Center*, Tennessee, AEDC-TR-75-114.
- Hsieh, T. (1977). Flow-field about a hemisphere cylinder at incidence. *Journal of Spacecraft and Rockets*, 14, 280-283.
- Mahomed, I., Roohani, H., Skews, B.W., & Gledhill, I.M.A. (2011). Unsteady shockwave dynamics in accelerating and decelerating flight. *The Aeronautical Journal*, 126, 401-423.
- Mahomed, I., Roohani, H., Skews, B.W., & Gledhill, I.M.A. (2023). Near-body shock wave motion for an accelerating slender body. *34th International Symposium on Shock Waves*. Daegu: Springer.
- Roohani, H., & Skews, B.W. (2009). The influence of acceleration and deceleration on shock wave movement on and around airfoils in transonic flight. *Shock Waves*, 19, 297-305.